Breakdown of Angular Momentum Selection Rules in High Pressure Optical Pumping Experiments

B. Lancor,[1] E. Babcock,[2] R. Wyllie,[1] and T. G. Walker[1]

[1]*Department of Physics, University of Wisconsin–Madison, Madison, Wisconsin 53706, USA*

[2]*Juelich Centre for Neutron Science, Garching 85747, Germany*

(Received 22 March 2010; published 20 August 2010)

We present measurements, by using two complementary methods, of the breakdown of atomic angular momentum selection rules in He-broadened Rb vapor. Atomic dark states are rendered weakly absorbing due to fine-structure mixing during Rb-He collisions. The effect substantially increases the photon demand for optical pumping of dense vapors.

DOI: 10.1103/PhysRevLett.105.083003 PACS numbers: 32.80.Xx, 32.70.−n, 33.55.+b

Optical pumping [1] of alkali-metal atoms at high temperatures and high buffer gas pressures is a powerful technique for precision spectroscopies (clocks, magnetometers, and masers) [2] and for production of hyperpolarized noble-gas nuclei by spin-exchange collisions [3]. Hyperpolarized noble-gas nuclei are extensively used as neutron spin filters [4] and targets for electron scattering [5], for magnetic resonance imaging [6] and nuclear magnetic resonance [7], and for fundamental studies [8]. For spin-exchange optical pumping, the small cross sections for spin exchange [3] are compensated for by operating at high alkali-metal densities, producing optical depths of $D \sim 100$. Such extreme opacities are managed by optically pumping the atoms into ''dark'' Zeeman levels that do not absorb the pumping light. Ideally, the vapor would become completely transparent to the pumping light, except for a small unpolarized layer near the cell walls. Including collisional spin-relaxation losses would lead to a modest linear attenuation of the pumping light as it propagates through the cell [3].

Under these extreme conditions the quality of the dark state becomes of great importance. In order to maintain high population of the dark state throughout the cell, the rate R at which unpolarized atoms at the entrance to the cell absorb pumping light must be $\sim D\Gamma$, where Γ is the spin-relaxation rate. Now suppose the dark-state atoms absorb the light at a small rate R_d. This directly increases the light absorption and also causes a small fraction of the atoms to populate strongly absorbing states. Under these conditions, the laser power required to optically pump the entire cell (the photon demand) increases by a factor [9] of

$$\Upsilon = 1 + 2R_d/\Gamma \approx 1 + 2DR_d/R. \quad (1)$$

For typical $D = 100$, a dark-state absorption rate of only $1/200$ of the unpolarized absorption rate doubles the photon demand. Previous experimental studies of spin-exchange optical pumping performance [9,10] invoked such dark-state absorption, without theoretical justification, to explain unexpectedly high photon demand.

In this Letter, we present the first direct observations of dark-state absorption due to fine-structure mixing in alkali-metal He collisions. We show that this light-induced spin-relaxation mechanism limits the attainable alkali-metal polarization and substantially increases the photon demand for optical pumping. While these collisions are well-studied in the context of line broadening [11] and fine-structure population transfer [12], prior line-shape studies were insensitive to how the collisions alter the angular momentum selection rules for light absorption [13].

The dark state for optical pumping of alkali-metal atoms with the light of photon spin projection $p = 1$ tuned to the first excited $^2P_{1/2}$ level is a fully nuclear (I) and electron (S) spin-polarized state with projection $m = S + I$. It follows from angular momentum conservation and the lack of an excited Zeeman sublevel of projection $m' = S + I + 1$ that excitation from the dark state is forbidden. In contrast, the increased angular momentum of a $^2P_{3/2}$ level allows no such dark state when pumping to that excited level [14].

Collisions with buffer gases alter the above simple argument since there are substantial shifts and mixing of the fine-structure levels [11], even for Rb and Cs atoms with large fine-structure splitting. This mixing appears in Fig. 1 as a divergence of the $|\Omega| = 1/2$ adiabatic potentials, Ω being the projection of the electronic angular momentum along the interatomic axis. This is equivalent to the $P_{1/2}$ state acquiring a small amount of $P_{3/2}$ character, allowing the atomic dark state to weakly absorb the pumping light. In addition, the strong repulsion between $^2S_{1/2}$ atoms and He in a collision produces a transient resonant absorption to the $|\Omega| = 3/2$ state of purely $^2P_{3/2}$ character at an interatomic distance of $8a_0$. Both of these effects lead to substantial absorption of the pumping light from the dark state in the atmospheric pressure cells typically used for these experiments. Thus, the usual atomic angular momentum selection rules are violated in Rb-He collisions.

We have measured the dark-state absorption cross section for Rb in the presence of ^{3}He gas of density [He] to be $\sigma_d = [\mathrm{He}] \times 1.10 \pm 0.12 \times 10^{-17}$ cm^2/amg [15] for light near the $^2S_{1/2} \rightarrow {}^2P_{1/2}$ (''$D1$'') resonance at a wavelength of 795 nm. This nearly frequency-independent absorption process competes with the resonantly enhanced

 © 2010 The American Physical Society

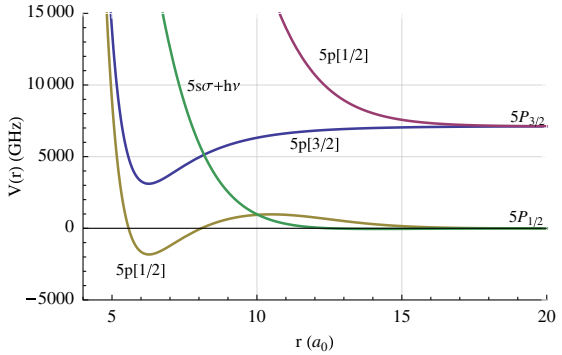

FIG. 1 (color online). Adiabatic energy curves for RbHe molecules [20] adapted to include fine structure [11]. The projection $|\Omega|$ of the total electronic angular momentum along the interatomic axis is given in brackets. The curve crossings between the photon-dressed $5s\sigma$ state and the two excited-state curves mean that photon absorption is allowed during a collision. These absorption processes violate the free-atom dipole selection rules, allowing normally angular momentum forbidden transitions to occur. The molecular absorption rates are nearly frequency-independent, so their impact on optical pumping is minimized with resonant narrow-band light that favors absorption between collisions.

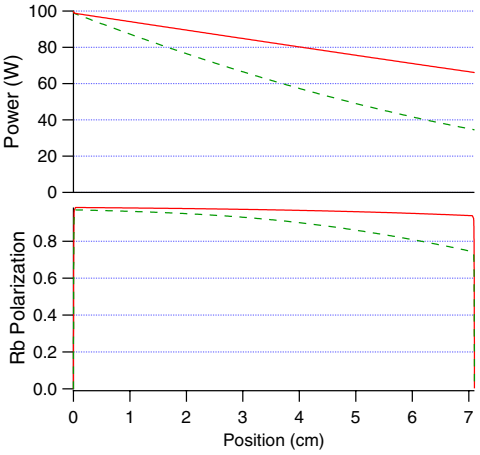

FIG. 2 (color online). Light propagation results with no (red, solid line) and measured (green, dashed line) dark-state absorption. The upper graph shows the power as a function of position. The dark-state absorption produces a faster attenuation of the light. The lower graph shows the Rb polarizations. The dark-state absorption reduces the Rb polarization at the cell entrance, with further reductions as the spectral profile of the light becomes increasingly off-resonant deeper inside the cell.

atomic absorption that obeys the usual atomic selection rules. Pumping with a narrowband laser tuned to the atomic resonance minimizes the relative contribution of the dark-state absorption. The bandwidth required can be estimated by using Eq. (1) to calculate the photon demand for a detuned monochromatic pump laser. With a pressure-broadened atomic line shape of width B'[He], the photon demand Υ doubles for light detunings of

$$\Delta = \sqrt{\frac{r_e f c B'}{4 D \sigma_d}} = 104\ \text{GHz}\sqrt{\frac{100}{D}}, \qquad (2)$$

where we have assumed $\Delta \gg B'$[He], and $B' = 18.7$ GHz/amg [13]. The oscillator strength is f, and r_e is the classical electron radius. Thus, light sources with widths exceeding 100 GHz will be very inefficient, consistent with experimental observation that narrowing of ~1000 GHz wide high power diode lasers to ~100 GHz results in substantial improvements in spin-exchange optical pumping [10].

Figure 2 illustrates the dark-state absorption effect, simulating the alkali polarization and laser power as a function of position in the cell, both with and without the dark-state absorption. We assume 100 W of pumping light with a 1000 GHz FWHM spectral profile, a 10 cm diameter, 7 cm long cell with 8 amg of ^{3}He and 0.066 amg of N_2, and $[\text{Rb}] = 4 \times 10^{14}$ cm^{-3}. Under these conditions we estimate a spin-relaxation rate of 630/s [10]. Without dark-state absorption the light is attenuated only due to ground-state spin relaxation, and only 35 W would be dissipated in the cell, maintaining a very high Rb polarization. When the dark-state absorption is taken into account the power dissipation per unit length is increased by a factor of $\Upsilon = 2.35$, as seen in Fig. 2, even at the entrance to the cell before the spectral hole is burned. The total power dissipation is much greater, now 65 W. The polarization drop is now quite substantial, reducing to 75% at the back of the cell. This is due to two effects: (i) The pumping rate is lower due to the greater power dissipation and the production of a complete hole in the spectral profile, and (ii) the remaining light is in the spectral region with low efficiency, further reducing the maximum attainable polarization. When the broadband source is replaced by a 100 GHz narrow-band source of half the power, Υ is reduced to 1.35 and high polarization is maintained throughout the cell.

We deduced the dark-state absorption cross sections by using the change in transmission of circularly polarized light through an optically pumped vapor as the atomic spin polarization is reversed. This is effectively a measurement of the circular dichroism of the vapor. Combining this with previous measurements of the absorption cross sections for unpolarized atoms [13] allows us to avoid a measurement of the Rb vapor pressure.

As shown in Fig. 3, a Rb vapor cell was optically pumped by a circularly polarized frequency-narrowed diode array bar [16]. A magnetic field of 50 G was applied in the pump propagation direction. A tunable probe external-cavity diode laser was attenuated to $P < 50$ μW, sent through a mechanical chopper operating at 485 Hz, and linearly polarized with a polarizing beam splitter cube. A portion was split off by a nonpolarizing beam splitter plate to provide a measure of the incident intensity, and the remainder was circularly polarized with a quarter wave plate. The probe beam propagated through the cell at an angle $\theta = 17.6°$ with respect to the magnetic field. The

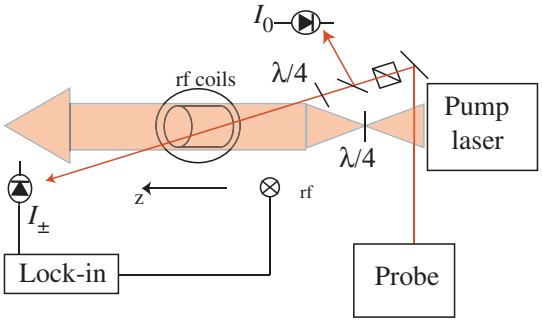

FIG. 3 (color online). Apparatus for measuring the circular dichroism of Rb-He vapor. The pump laser, propagating parallel to a magnetic field B_z, spin-polarizes Rb atoms either parallel or antiparallel to the field. The fractional transmission of a weak, circularly polarized, tunable probe laser is determined by the ratio of photodiode voltages before and after the cell. The circular dichroism is then determined from the transmissions for both directions of Rb polarization. The absolute Rb polarization is determined by driving rf resonances with field $B_{\rm rf}$ and measuring the resulting modulated Faraday rotation of the probe laser.

incident and transmitted intensities were sent to lock-in amplifiers referenced to the chopper frequency. To change the direction of the atomic spin polarization, the pump $\lambda/4$ plate was rotated 90°. To obtain the relation between the incident and transmitted intensities in the absence of Rb (thus accounting for loss in the windows of the oven and cell), a measurement was taken at room temperature.

Two natural abundance Rb cells were used in this experiment. The low pressure cell is a closed 4.9 cm long cylinder, with 0.80 amg ^{3}He and 0.07 amg of N_2. The high pressure cell is a blown GE180 sphere of diameter 3.5 cm, filled with 3.27 amg of ^{3}He and 0.13 amg N_2. The cell being studied was placed in a temperature-controlled flowing hot air oven. Temperatures ranging from ~60 to ~180 °C, corresponding to $[\mathrm{Rb}] = 1\text{–}200 \times 10^{12}$ cm^{-3}, were used to produce appropriate optical thickness for transmission measurements at a range of frequencies.

The Rb spin polarization P was measured with transverse EPR spectroscopy [17,18]. As the holding field was swept through the EPR resonances, the resulting polarization modulation of the probe beam was measured by a polarizer and a fast photodetector. The spin polarization was deduced by using the area ratio method [17].

The basic parameters observed by the experiment are the transmissions $I_\pm$ for circularly polarized probe light propagating at angle θ to the spin polarization $\pm P$. The absorption cross section is [9,19]

$$\sigma(\pm) = \sigma_0(1 \mp P_\infty P \cos\theta), \tag{3}$$

where P_∞, the normalized circular dichroism of the vapor, would be 1 in the absence of the dark-state absorption. We extract P_∞ from the transmitted intensities $I_\pm = I_o \exp\{-[\mathrm{Rb}]\sigma(\pm)l\}$ by finding

$$\frac{-\ln(I_-/I_o) + \ln(I_+/I_o)}{-\ln(I_-/I_o) - \ln(I_+/I_o)} = PP_\infty \cos\theta. \tag{4}$$

The dark-state absorption cross section σ_d is $\sigma(+)$ evaluated at $\theta = 0$ and $P = 1$:

$$\sigma_d = \sigma_0(1 - P_\infty). \tag{5}$$

We combine our measurements of P_∞ with recent spin-independent pressure-broadened cross sections [13] σ_0 to obtain σ_d.

The measured P_∞ in the vicinity of the fine-structure resonances is shown for both cells in Fig. 4. A very important result from Fig. 4 is the agreement between the two cells, despite their very different He pressures. At detunings outside the atomic linewidth of 15–60 GHz [13], σ_0 is proportional to the He pressure. Thus, only if σ_d is also proportional to the He pressure will the dichroism be pressure-independent. The agreement between the two cells at different pressures thus confirms the source of the impure dichroism as being Rb-He collisions. Other systematic checks of hyperfine effects, off-resonant pumping, and N_2 contributions will be presented in a subsequent publication. The solid line in the inset in Fig. 4 corresponds to $\sigma_d/[\mathrm{He}] = 1.10 \pm 0.12$ cm^2/amg at the $D1$ resonance. This value was used in the simulation of Fig. 2, which shows the dramatic effect of the breakdown of atomic selection rules on optical pumping of optically thick vapors.

As a second, quite different, method for measuring P_∞ at frequencies off the $D1$ resonance, we used a 30 W frequency-narrowed external-cavity laser [16] to optically pump the atoms at different frequencies ν. The equilibrium polarization attained by using optical pumping with the light of normalized circular dichroism P_∞ is

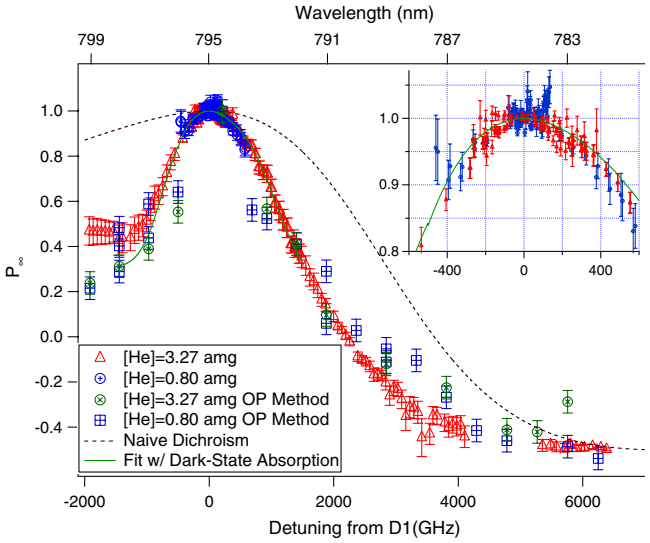

FIG. 4 (color online). Normalized circular dichroism results near the $5S$-$5P$ resonance lines of Rb. The agreement between cells of different He pressure verifies that the effect originates from absorption in Rb-He collisions. The solid line shows the frequency dependence of the dichroism due to the dark-state absorption. Inset: Circular dichroism in the critical region near the $D1$ line.

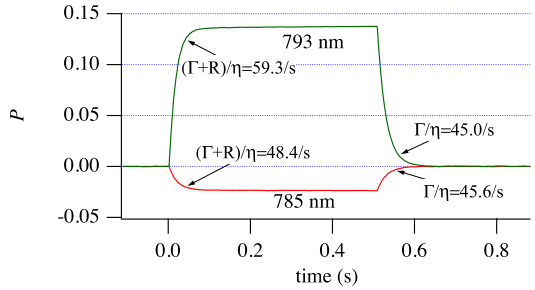

FIG. 5 (color online). Pumping/decay transients used to measure P_∞. Narrow-band pumping light is turned on at $t = 0$, and the polarization builds up to the steady-state value of Eq. (6). The exponential buildup and decay constants allow the pumping rate R and the relaxation rate Γ to be measured. Note that the sign of the polarization is opposite for 785 nm pumping as compared to 793 nm pumping, due to the dichroism of the vapor being negative for the former case.

$$P(\nu) = P_\infty(\nu)\frac{R(\nu)}{R(\nu)+\Gamma}. \quad (6)$$

Thus, by measuring $P(\nu)$, pumping rate $R(\nu)$, and spin-relaxation rate Γ, we deduce P_∞.

We chopped the pumping laser with a mechanical shutter and measured the spin polarization as a function of time, as illustrated in Fig. 5, by using Faraday rotation. For small polarizations, the rising transient builds up polarization to the steady-state value (6) at a rate $[R(\nu)+\Gamma]/\eta$, and the falling transient decays at the rate Γ/η, where the slowing-down factor $\eta = 10.8$ for natural abundance Rb [18]. The Faraday rotation was calibrated by EPR spectroscopy.

The deduced values of P_∞ by using this optical pumping (OP) method are shown in Fig. 4 and agree with the results of the direct dichroism measurements. With the OP method, the zero crossing of the dichroism is particularly dramatic as the signal of Fig. 5 reverses sign near 790 nm. A naive pressure broadening model that neglects the angular momentum altering properties of Rb-He collisions would predict the zero crossing to occur at 787.5 nm.

We have also measured $\sigma_d = [N_2] \times 1.49 \pm 0.15 \times 10^{-17}$ cm^2/amg for Rb-N_2 collisions. The near equality of σ_d for He and N_2 is in stark contrast to the factor of 180 ratio of fine-structure changing collisions for the two species. This emphasizes that the mixing effects studied here are sensitive to different aspects of the atom-atom interactions as compared to fine-structure changing collisions.

In summary, we used two distinct methods to demonstrate the breakdown of atomic angular momentum selection rules due to buffer gas collisions. This breakdown compromises the atomic dark state and has dramatic effects on the performance of optical pumping experiments with dense vapors. This Letter shows for the first time how to extend the standard model of Ref. [3] to account for the light-induced relaxation effects seen in recent experiments [9,10]. The results explain the substantial observed improvements in spin-exchange optical pumping using narrow-band light sources.

We benefited from discussions with T. Gentile. This work was supported by the DOE, Basic Energy Sciences.

[1] W. Happer, Rev. Mod. Phys. **44**, 169 (1972); W. Happer, Y.-Y. Jau, and T. G. Walker, *Optically Pumped Atoms* (Wiley, New York, 2009).
[2] Y.-Y. Jau, N. N. Kuzma, and W. Happer, Phys. Rev. A **69**, 061401 (2004); I. K. Kominis, T. W. Kornack, J. C. Allred, and M. V. Romalis, Nature (London) **422**, 596 (2003); A. G. Glenday, C. E. Cramer, D. F. Phillips, and R. L. Walsworth, Phys. Rev. Lett. **101**, 261801 (2008).
[3] T. Walker and W. Happer, Rev. Mod. Phys. **69**, 629 (1997).
[4] T. Gentile, W. Chen, G. Jones, E. Babcock, and T. Walker, J. Res. Natl. Inst. Stand. Technol. **110**, 299 (2005); E. Babcock, S. Boag, M. Becker, W. C. Chen, T. E. Chupp, T. R. Gentile, G. L. Jones, A. K. Petukhov, T. Soldner, and T. G. Walker, Phys. Rev. A **80**, 033414 (2009).
[5] J. Singh, P. Dolph, K. Mooney, V. Nelyubin, A. Tobias, A. Kelleher, T. Averett, and G. Cates, in *SPIN PHYSICS: 18th International Spin Physics Symposium* (AIP, New York, 2009), Vol. 1149, p. 823; K. Slifer *et al.* (Jefferson Lab E94010 Collaboration), Phys. Rev. Lett. **101**, 022303 (2008).
[6] J. H. Holmes, R. L. O'Halloran, E. K. Brodsky, Y. Jung, W. F. Block, and S. B. Fain, Magn. Reson. Med. **59**, 1062 (2008).
[7] X. Zhou, D. Graziani, and A. Pines, Proc. Natl. Acad. Sci. U.S.A. **106**, 16 903 (2009).
[8] S. W. Morgan, B. V. Fine, and B. Saam, Phys. Rev. Lett. **101**, 067601 (2008); G. Vasilakis, J. M. Brown, T. W. Kornack, and M. V. Romalis, *ibid.* **103**, 261801 (2009).
[9] E. Babcock, I. Nelson, S. Kadlecek, B. Driehuys, L. W. Anderson, F. W. Hersman, and T. G. Walker, Phys. Rev. Lett. **91**, 123003 (2003).
[10] W. C. Chen, T. R. Gentile, T. G. Walker, and E. Babcock, Phys. Rev. A **75**, 013416 (2007).
[11] N. Allard and J. Kielkopf, Rev. Mod. Phys. **54**, 1103 (1982).
[12] M. D. Rotondaro and G. P. Perram, Phys. Rev. A **58**, 2023 (1998); L. Krause and E. S. Hrycyshyn, Can. J. Phys. **48**, 2761 (1970).
[13] M. V. Romalis, E. Miron, and G. D. Cates, Phys. Rev. A **56**, 4569 (1997).
[14] W. Happer and W. A. van Wijngaarden, Hyperfine Interact. **38**, 435 (1987).
[15] 1 amg $= 2.69 \times 10^{19}$ cm^{-3}.
[16] E. Babcock, B. Chann, I. Nelson, and T. Walker, Appl. Opt. **44**, 3098 (2005).
[17] A. B. Baranga, S. Appelt, C. J. Erickson, A. R. Young, and W. Happer, Phys. Rev. A **58**, 2282 (1998).
[18] S. Appelt, A. B. Baranga, C. J. Erickson, M. Romalis, A. R. Young, and W. Happer, Phys. Rev. A **58**, 1412 (1998).
[19] B. Chann, E. Babcock, L. W. Anderson, and T. G. Walker, Phys. Rev. A **66**, 033406 (2002).
[20] J. Pascale, Phys. Rev. A **28**, 632 (1983).